

# Microstructure, Hardness and Wear Rate of A356 Aluminium Alloy Surface Alloyed with Nitrided Titanium using GTA

R. Saravanan\*, S. Srihari, A. Arvind, P. Sreeranj, K. S. Dheeraj, R. Sellamuthu and Sanjivi Arul

Department of Mechanical Engineering, Amrita School of Engineering - Coimbatore, Amrita Vishwa Vidyapeetham University, Coimbatore - 641 112, Tamil Nadu, India; r\_saravanan@cb.amrita.edu, sriharisury@gmail.com, arvind.ajayakumar@gmail.com, sreeranjpranju@gmail.com, dheerajks.2301@gmail.com, r\_sellamuthu@cb.amrita.edu, s\_arul@cb.amrita.edu

## Abstract

**Background/Objectives:** The study aims to improve surface properties of aluminium A356 alloy by surface alloying it with nitrided titanium, in a nitrogen environment, using Gas Tungsten Arc (GTA) as heat source. **Methods/Statistical Analysis:** Nitrided titanium sheets were surface alloyed with cast aluminium A356 blocks, in nitrogen environment, with GTA as heat source for melting. The cross-sectional microstructure of the specimens was studied using inverted metallurgical microscope. Further analysis was carried out using SEM/EDS to identify the formation of nitrides and intermetallic compounds. The hardness of the specimens was measured using Vickers hardness tester and the wear rate was determined using pin-on-disc wear tester. **Findings:** Microstructure analysis revealed a uniform and granular refined structure in the modified layer compared to the coarse and dendritic structure of the cast block. EDS analysis indicated the formation of hard-intermetallic compounds. The hardness was measured to be highest at the surface of the central fusion zone, with a maximum value of 656 HV while as-cast aluminium block exhibited only 76 HV. The measured wear rate was  $10 \times 10^{-4}$  mm<sup>3</sup>/m for the modified layer, compared to  $52 \times 10^{-4}$  mm<sup>3</sup>/m of the substrate. Alongside, the loss in weight after wear dropped by 4 mg. The coefficient of friction of the modified surface showed a constant trend during the wear-off period. The enhancement in these surface properties is attributed to the formation of nitrides and other intermetallic compounds that in the modified layer during surface alloying. Additionally, the use of GTA as heat source renders the surface alloying process to be economically feasible relative to other employable methods. **Applications/Improvements:** The devised surface alloying method used to enhance the surface properties of A356 is cheap, flexible and effective and finds intensive application in marine, automotive and manufacturing sectors.

**Keywords:** A356, Gas Tungsten Arc, Hardness, Nitriding, Surface Alloying, Titanium, Wear Rate

## 1. Introduction

Of all the grades of aluminium, alloy A356 continues its popularity for its dimensionally accurate castability properties such as fluidity and tightness, mechanical strength, corrosion resistance, machinability, weldability and finish. Besides its well-known applications in the automobile sector for wheel rims, cylinder blocks & heads, truck chassis and spring brackets, the other common interested industries are the marine sector for its hardware, aerospace sector for aircraft wheels, pump parts & fuel tank elbows and the civil sector for its bridge

railing parts<sup>1</sup>{Jayakumar, 2014 #26}{Jayakumar, 2014 #26}. Yet, similar to other aluminium alloys, A356 suffers with low surface hardness and poor wear resistance properties.

To cater to the industries' demand for metals with high hardness, corrosion and wear resistance, among others, literature has grown extensively with a tremendous focus on improving surface characteristics of metals. With aluminium alloys being virile nitride formers, surface nitriding has been explored extensively by researchers and industries, citing its improved hardness and wear resistance properties over the untreated surfaces<sup>2-5</sup>. In

\* Author for correspondence

this regard, there have been extensive works on the most recognized titanium nitride (TiN) coatings, which grew as an attractive field of research and development<sup>6</sup>. However, in the past decade, aluminium titanium nitride (AlTiN) has supplanted TiN in many applications, given its attractive advantage of concealing inward oxygen diffusion by forming a highly adhesive and protective Al<sub>2</sub>O<sub>3</sub> film<sup>7</sup>. AlTiN layers are found to have high hardness, good thermal coefficient, high abrasive wear and corrosion resistance and in general, excellent properties even at high temperatures<sup>8-11</sup>. Its application in the form of coatings on tools and dies have been attributed to these properties. Though it is well-known for its tribological usefulness, recent studies have explored its uses in other areas as well<sup>12</sup>.

It was found from literature that surface alloying titanium nitride over aluminium, in the expectation to form AlTiN, has not yet been explored. In literature, surface alloying has been widely carried out using a variety of other techniques such as PVD, CVD, Electron Beam processing, Laser surface cladding, Ion plate deposition and Thermal spraying and many of its derivatives. However, costly initial investments, expensive processing costs and requisites such as vacuum are setbacks for their application<sup>13</sup>. GTA as a technique for surface alloying was introduced<sup>14</sup>, in which heat energy supplied by the electric arc between the tungsten electrode and substrate is used for alloying. GTA technique for surface alloying is flexible, fast, precise and economical in terms of input power, time and material. TIG torch was suggested for aluminium nitriding<sup>15</sup> and in<sup>16</sup> showed GTA as an alternative heat source for surface refining. Yet, related works are limited<sup>17,18</sup>. Combining these findings from literature, GTA was chosen as the heat source for carrying out the surface alloying in this current work.

Alloying aluminium and titanium requires high heat input owing to the high thermal conductivity of aluminium<sup>19</sup>. At the same time, previous studies showed that alloying at higher energy rates has retarding effects on the hardness and wear properties<sup>17,20</sup>. In this case, the heat input is characterized by the parameters used to establish the GTA heat source, namely operating current, voltage, electrode diameter, electrode travel speed, electrode-tip distance and tip angle. Rather than continuous GTA alloying, optimized parameters ensure higher weld strength with improved properties at lower heat input and high cooling rate<sup>21,22</sup> worked to establish a model that

helped determine the optimal parameters. Along these lines, in the present work, the optimized values<sup>23</sup> were considered for carrying out the alloying process.

Hence, paper presents the study of surface modification of A356 aluminium alloy by surface alloying nitrided titanium sheet onto its surface in the presence of nitrogen atmosphere using GTA as the source of heat. The corresponding microstructural features were studied. To determine the improved performance characteristics of the surface modified specimen, the traditional microhardness and wear tests were performed and the results were compared with that of as-cast A365 alloy. The details of the tests and results are presented in the following sections.

## 2. Experimental Procedure

### 2.1 Surface Alloying

Commercially available A356 Aluminium ingots were purchased and tested using arc atomic emission spectroscopy to reveal the chemical compositions of the elements present, as given in Table 1.

These ingots were cast into rectangular blocks using green sand mold casting, which were then machined to the dimensions of 150×30×30 mm bars and used as the substrate. The specimens were abraded using SiC sheet to ensure greater adhesion. Unalloyed Commercially Pure (CP) titanium Grade 2 (99.2%) sheets of 0.4 mm thickness was chosen for the surface alloying process, considering its typical use for airframe & aircraft engine parts and marine components<sup>24</sup>. Also, its usage in the form of sheets would facilitate a more uniform coating and ease the surface alloying process. Initially, six 150×50 mm sheets of titanium were heat treated at a temperature of 650°C in nitrogen environment to form a nitride coating over them. The first piece was nitrided for 1 hr, the second one for 2 hrs and so on till the sixth piece was removed after 6 hrs of nitriding. However, the sheets heat treated for 5 hrs and 6 hrs were discarded due to extreme brittleness owing to excessive nitride formation. The heat treated sheets were placed on A356 Aluminium substrate and surface processing was carried out using a LINCOLN Invertec® V205-T AC/DC TIG Welder Figure1 in DCEN configuration. The processing parameters were fixed by maintaining an arc discharge current of 150 A, electrode travel speed of 2 mm/s and tip angle of 180°. A  $\phi$ 2.4 mm non-consumable 2% thoriated tungsten electrode was

used and maintained at a workpiece to electrode-tip distance of 3mm. With nitrogen being a diatomic gas with high ionization temperature, argon gas was used to strike the initial arc. The supply was later switched over to a mixture of ultra-high purity (99.999%) nitrogen gas and argon gas, which was supplied at a constant standard pressure of 1bar, corresponding to a flow rate of 18 L/min (approx.). The surface melting was continued in this mixture atmosphere ( $N_2/Ar$  ratio of 1:1) to avoid undesirable effects on the electric arc as well as to ensure maximum nitriding.



**Figure 1.** Experimental setup used for surface alloying.

**Table 1.** Chemical composition of A356 Aluminium alloy

Element	Si	Fe	Cu	Mg	Ti	Al
Wt %	8.11	0.251	0.5	0.405	0.102	balance

## 2.2 Microstructure

To prepare the nitrided samples for the microstructural analysis, initially, they were cut perpendicular to the alloyed surface. Then, the cross-sectional surfaces were polished using corundum emery papers, followed by diamond polishing suspensions. Finally, the surfaces were chemically etched using Keller's reagent to reveal the microstructural features. Subsequently, the corresponding microstructures were examined using an inverted metallurgical microscope (Model: ZEISS Axiovert 25CA). To determine the elemental constituents, the alloyed regions were characterized by observing them under a scanning optical microscope (Model: ZEISS Merlin SEM), operated at an acceleration voltage of 15 kV, kit up with an energy-dispersive spectral (EDS) analyzer.

## 2.3 Hardness Test

To determine the microhardness of the cross-section of the modified surface, MITUTOYO (HM-210) Vickers Hardness Tester was used to carry out the tests under a

constant applied load of 100 g for a dwell time of 15 s. The microhardness was measured along the width and depth of the modified layer.

## 2.4 Wear Test

The abrasive wear property of the modified surface was determined using a DUCOM pin-on-disc wear tester. Cylindrical pins of  $\phi 12$  mm prepared from as-cast and alloyed samples were tested, under the parameters listed in Table 2, without lubrication. A hardened steel disc plate of 60 HRC hardness served as the Ra 0.15  $\mu\text{m}$  rough abrasive counter-face. The wear resistance was then evaluated using both theoretical wear rate calculation and experimental wear weight loss method.

**Table 2.** Wear test parameters

S.No.	Parameter	Value	Units
1	Axial Load	20	N
2	Sliding distance	1500	m
3	Rotational speed	424	rpm
4	Track diameter	110	mm

## 3. Results and Discussion

In this section, the best results of the experimentation and the corresponding justifications have been presented.

### 3.1 Microstructure

Figure 2 shows the optical micrograph of the cross-sectional view showing the hemispherical interface of the alloyed layer and the substrate. Compared to the substrate, the near-smooth alloyed layer revealed a microcrack-free surface. With the depth of the alloyed layer being about 4 mm, the interface also revealed that a homogeneous and good adhesive layer has been formed.

Shown in Figure 3 is a typical cross-sectional view of a surface alloyed specimen free from cracks or porosity. The absence of any discernible defects indicates near-complete melting and bonding. Figure 3(a) shows the microstructure of the as-cast A356 aluminium alloy substrate revealing an overall coarse grained and dendritic structure. Figure 3(b) shows the modified cross-sectional region which is observed to be composed of a more uniform and refined granular structure. This refinement was attributed to the rapid solidification that ensues the high rate of heat transfer and thermal gradient between the melt region and substrate<sup>25</sup>.

Figure 4 and Figure 5 show the SEM morphology of the alloyed layer and the EDS analysis of the indicated regions respectively. The elemental analysis of region A in Figure 4 showed aluminium, titanium, silicon and nitrogen having large peaks (Figure 5(a)). Hence, it was adjudged that nitride compounds of Al-Ti-N / Ti-Si-N / Ti-N / Al-N / Si-N were formed. This feasibility was attributed to the strong nitride forming titanium, aluminium and silicon that combined with the dissolved nitrogen during solidification. The ternary and phase diagrams of the corresponding combinations also support the prediction. Figure 5(b) corresponding to region B in Figure 4 showed peaks from aluminium and titanium without any notable amount of nitrogen and hence, the formation of an intermetallic compound of Al-Ti, during solidification, was considered. Though these possibilities were inferred, their phases have to be identified with an X-ray diffraction (XRD) analysis. The trace presence of oxygen can be due to the oxidation of aluminium during the grinding and polishing processes. The microstructural refinement can also be attributed to the formation of these compounds at the surface layer.

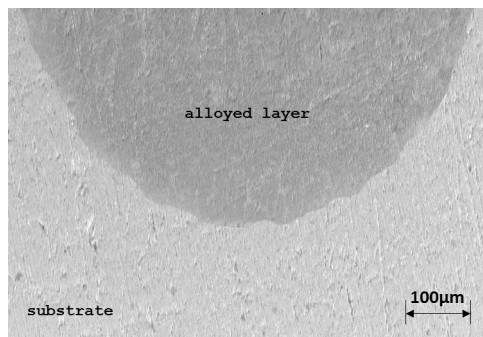
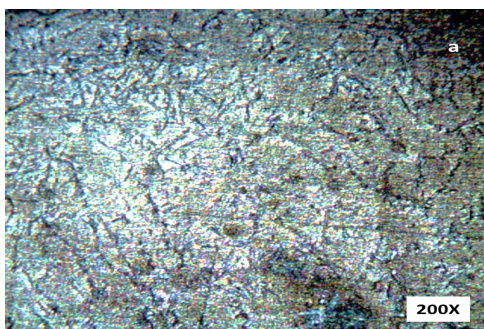
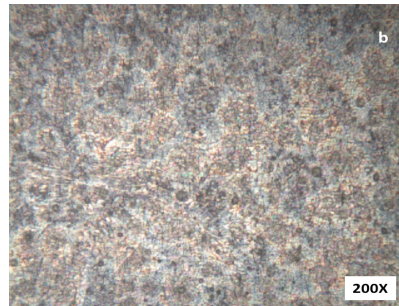


Figure 2. Optical micrograph of alloyed layer/ substrate interface.



(a)



(b)

Figure 3. Optical cross-sectional microstructure (a) substrate (b) modified zone.

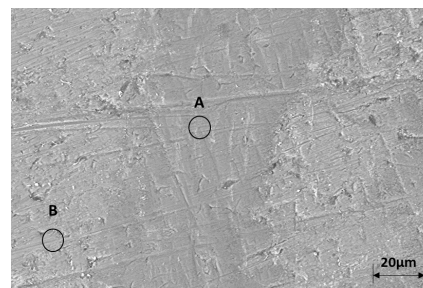
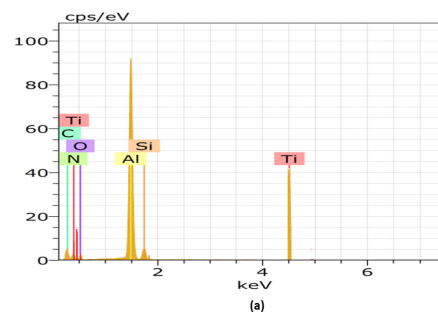
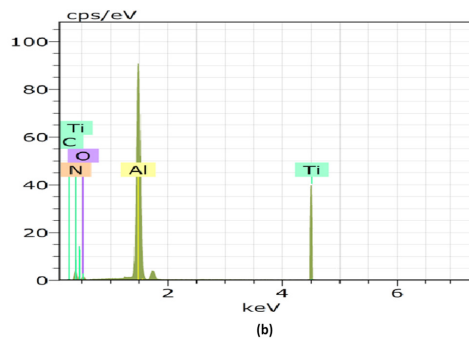


Figure 4. SEM micrograph of alloyed layer.



(a)



(b)

Figure 5. Elemental distribution of zones indicated A and B in Figure-4 respectively.

### 3.2 Hardness

The variation of the measured microhardness along the width and depth of the modified layer are shown graphically in Figure 6 and Figure 7 respectively. In Figure 6, the hardness value was seen to be highest in the central fusion zone than that in the heat affected zone (HAZ) and substrate. The hardness strikes a peak value of 650 HV at the center and gradually drops along either sides.

In Figure 7, the vertical hardness gradient along the depth of the melt region observed a decreasing trend as hardness gradually decreases from the maximum hardness value of 656 HV at the surface to 118 HV at the melt depth.

The maximum recorded hardness of the alloyed surface was about 656 HV, being much harder than the substrate aluminium, which possessed about 76 HV. Such substantial increase in hardness is because of the formation of the hard nitrides and intermetallic Al-Ti in the surface modified layer. The refined microstructure of the region reaffirms the same. The maximum hardness near the center of the alloyed layer is due to the increased concentration of these compounds in this layer. Without any other works on surface alloying of titanium nitride on aluminium alloy, this hardness increase could not be compared.

The varying hardness profile is due to the non-uniform distribution of the nitrides and the intermetallic Al-Ti in the cross-section. Along the width, the increased concentration of compounds at the center can be explained by the Gaussian energy distribution of the GTA that generates higher temperature at the center than at the sides. Due to this, absorption of nitrogen and penetration of titanium decreases alongside the center. The direct dependency of hardness with the concentration of dissolved nitrogen and the effective alloying of titanium explains the profile Figure 6. Along the depth, with decreasing heat energy, lower diffusion of nitrogen and lower penetration of titanium at deeper layers of molten pool results in its profile Figure 7. Additionally, in general, the faster cooling rate at the substrate interface inhibits the growth of these compounds<sup>26</sup>. Besides, the diverse compounds exhibit their respective hardness properties, which adds to the variation.

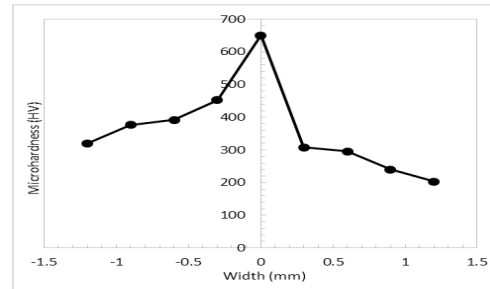


**Figure 6.** Hardness profile of nitrided region along the width direction of modified layer.

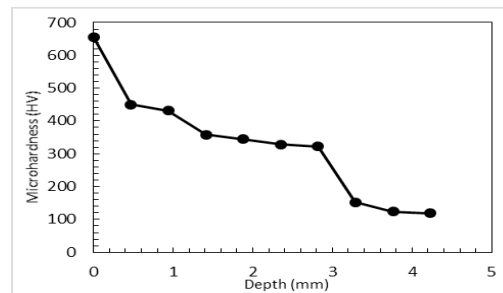


**Figure 7.** Hardness profile of nitrided region along the depth direction of modified layer.

### 3.3 Wear Test

The wear resistance of the surface modified layer was determined from the variation of the wear with sliding time as shown in Figure 8. The wear rate of the treated surface was as low as  $10 \times 10^{-4} \text{ mm}^3/\text{m}$ . This is lower than the  $52 \times 10^{-4} \text{ mm}^3/\text{m}$  of the substrate.

A further substantiation of the improved wear resistance was observed with the drop in weight loss from 7 mg to 3 mg after sliding a distance of 1500m Table 3.

The variation of coefficient of friction (CoF) with time, from Figure 9, initially showed slight irregular variations with a mean coefficient of about 0.6. However, nearly after 150s, it traced a more regular and invariant value of about 0.9 throughout the rest of the wear-off period. Such a profile indicates a constant metal-metal contact and shows enhanced wear properties<sup>27</sup>.

The worn surfaces of the as-cast aluminium and the alloyed surface are shown in Figure 10. The abrasive wearing of the unalloyed surface left deep grooves as an indication of the plastic deformation it had undergone. In contrast, the alloyed surface exhibited a relatively smoother

surface with the reduced severity and shallowness of the grooves and scars. This implied that it had worn far lesser than the as-cast aluminium. As with hardness, this improvement in wear resistance of the alloyed surface is yet again due to the presence of the formed hard nitrides and intermetallic Al-Ti.



Figure 8. Variation of wear with sliding time.

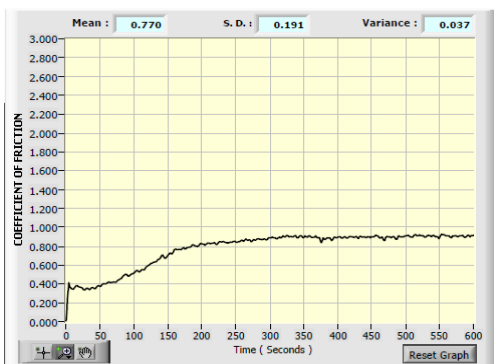
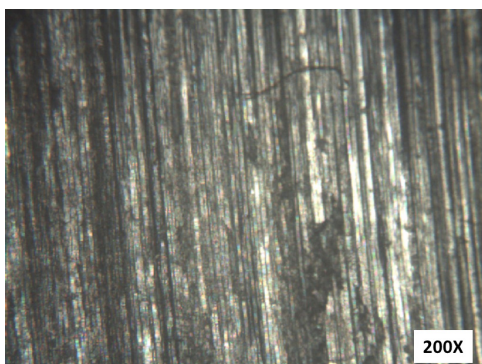
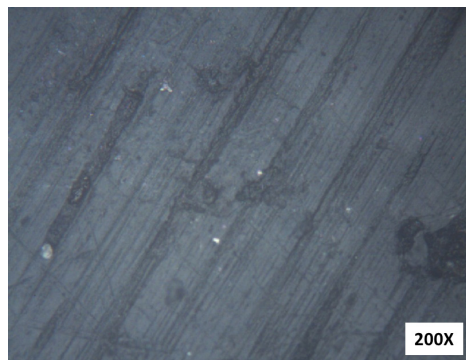


Figure 9. Coefficient of friction versus time.



(a)



(b)

Figure 10. Wear debris of (a) as-cast aluminium (b) modified surface.

Table 3. Wear weight loss

Sample	Weight before test (g)	Weight after test (g)	Weight loss (g)
As-cast	7.995	7.988	0.007
Alloyed surface	7.756	7.753	0.003

## 4. Conclusion

Surface modification of A356 aluminium alloy was carried out to improve its surface characteristics. The surface alloyed specimens were studied for their microstructural, hardness and wear characteristics. A refined grain structure was observed in the modified region over the coarse structure in the unaffected substrate. EDS analysis helped identify the formation of nitrides and intermetallic Al-Ti. The maximum hardness was recorded as 656 HV, greater than that of the substrate which possessed 76 HV. The wear resistance also improved with a reduction in wear rate from  $52 \times 10^{-4} \text{ mm}^3/\text{m}$  to  $10 \times 10^{-4} \text{ mm}^3/\text{m}$ . Additionally, weight lost due to wear decreased by 4 mg. CoF remained almost constant throughout the wear-off period. With decreased wear, the modified surface showed a relatively smoother worn surface. The increase in the hardness and wear resistance was attributed to the formation of hard nitrides and intermetallic Al-Ti present in the modified layer.

## 5. References

1. Kaufman JG, Rooy EL. Aluminum alloy castings: properties, processes, and applications: Asm International. 2004.

2. Richter E, Gunzel R, Parasacandola S, Telbizova T, Kruse O, Moller W. Nitriding of stainless steel and aluminium alloys by plasma immersion ion implantation. *Surface and Coatings Technology*. 2000 Jun; 128:21–7.
3. Chen HY, Stock HR, Mayr P. Plasma-assisted nitriding of aluminum. *Surface and coatings technology*. 1994 Jun; 64(3):139–47.
4. Kaczmarek L, Sawicki J, Kyziol K, Siniarski D, Jonas S, Steglinski M. Surface modification of aluminium-lithium alloy using prenitriding option and SixNy coating deposition. *Journal of Achievements in Materials and Manufacturing Engineering*. 2009; 37(2):282–5.
5. Meneau C, Andrezza P, Andrezza-Vignolle C, Goudeau P, Villain JP, Boulmer-Leborgne C. Laser surface modification: structural and tribological studies of AlN coatings. *Surface and Coatings Technology*. 1998 Mar; 100:12–6.
6. Sundgren JE. Structure and properties of TiN coatings. *Thin solid films*. 1985; 128(1):21–44.
7. Hsieh J, Liang C, Yu C, Wu W. Deposition and characterization of TiAlN and multi-layered TiN/TiAlN coatings using unbalanced magnetron sputtering. *Surface and Coatings Technology*. 1998 Sep; 108:132–7.
8. Munz WD. Titanium aluminum nitride films: A new alternative to TiN coatings. *Journal of Vacuum Science and Technology A*. 1986 Apr; 4(6):2717–125.
9. Zukerman I, Raveh A, Kalman H, Klemberg-Sapieha J, Martinu L. Thermal stability and wear resistance of hard TiN/TiCN coatings on plasma nitrided PH15-5 steel. *Wear*. 2007 Sep; 263(7):1249–52.
10. Sproul WD, Legg KO. *Advanced surface engineering: opportunities for innovation*: Technomic. 1995.
11. Bressan J, Hesse R, Silva E. Abrasive wear behavior of high speed steel and hard metal coated with TiAlN and TiCN. *Wear*. 2001 Oct; 250(1):561–8.
12. Brogren M, Harding GL, Karmhag R, Ribbing CG, Niklasson GA, Stenmark L. Titanium–aluminum–nitride coatings for satellite temperature control. *Thin Solid Films*. 2000 Jul; 370(1):268–77.
13. Liang W, Zhao X. Improving the oxidation resistance of TiAl-based alloy by siliconizing. *Scripta materialia*. 2001; 44(7):1049–54.
14. Wenbin D, Haiyan J, Xiaoqin Z, Dehui L, Shoushan Y. Microstructure and mechanical properties of GTA surface modified composite layer on magnesium alloy AZ31 with SiC P. *Journal of Alloys and Compounds*. 2007 Feb; 429(1):233–41.
15. Hioki S, Yamada T, Hatano K, Haneda M, Imanaga S. Method for melt nitriding of aluminum or its alloy. *Google Patents*; 1981 Jan.
16. Saravanan R, Sellamuthu R. An Investigation of the Effect of Surface Refining on the Hardness and the Wear Properties of Al-Si Alloy. *Applied Mechanics and Materials; Trans Tech Publ*. 2014 Jul; 53–7.
17. Heydarzadeh Sohi M, Ansari M, Ghazizadeh M, Zebardast H. Liquid phase surface nitriding of aluminium using TIG process. *Surface Engineering*. 2014 Dec; 31(8):598–604.
18. Zheng X, Ren Z, Li X, Wang Y. Microstructural characterization and mechanical properties of nitrided layers on aluminum substrate prepared by nitrogen arc. *Applied Surface Science*. 2012 Oct; 259:508–14.
19. Kou S. *Welding Metallurgy* 2nd edn. 2nd edition John Wiley & Sons, New Jersey, USA. 2003.
20. Dyuti S, Mridha S, Shaha S. Surface modification of mild steel using tungsten inert gas torch surface cladding. *American Journal of Applied Sciences*. 2010 Jun; 7(6):815–22.
21. Sivachidambaram P, Balachandar K. Optimization of Pulsed Current TIG Welding Parameters on Al-SiC Metal Matrix Composite-An Empirical Approach. *Indian Journal of Science and Technology*. 2015 Sep; 8(23):1–7.
22. Arul S, Sellamuthu R. Application of a simplified simulation method to the determination of arc efficiency of Gas Tungsten Arc Welding (GTAW) and experimental validation. *International Journal of Computational Materials Science and Surface Engineering*. 2011; 4(3):265–80.
23. Saravanan R, Sellamuthu R. Determination of the Effect of Si Content on Microstructure, Hardness and Wear Rate of Surface-refined Al-Si Alloys. *Procedia Engineering*. 2014 Dec; 97:1348–54.
24. Boyer R, Welsch G, Collings E. *Materials Properties Handbook: Titanium Alloys*. ASM International, Materials Park, USA. 1994.
25. Teker T. Effect of synergic controlled pulsed and manual gas metal ARC welding processes on mechanical and metallurgical properties of AISI 430 ferritic stainless steel. *Archives of Metallurgy and Materials*. 2013 Dec; 58(4):1029–35.
26. Mridha S. Titanium nitride layer formation by TIG surface melting in a reactive environment. *Journal of Materials Processing Technology*. 2005 Oct; 168(3):471–7.
27. Stott F, Mitchell D, Wood G. The influence of temperature on the friction and wear of thin ceramic coatings in carbon dioxide. *Journal of Physics D: Applied Physics*. 1992 Jan; 25(1A):189–94.